

# Temporal Alignment for History Representation in Reinforcement Learning

Aleksandr Ermolov\*, Enver Sangineto<sup>† §</sup> and Nicu Sebe\*

\*Department of Information Engineering and Computer Science (DISI), University of Trento, Italy

<sup>†</sup>Department of Engineering (DIEF), University of Modena and Reggio Emilia, Italy

Email: aleksandr.ermolov@unitn.it

**Abstract**—Environments in Reinforcement Learning are usually only partially observable. To address this problem, a possible solution is to provide the agent with information about the past. However, providing complete observations of numerous steps can be excessive. Inspired by human memory, we propose to represent history with only important changes in the environment and, in our approach, to obtain automatically this representation using self-supervision. Our method (TempAI) aligns temporally-close frames, revealing a general, slowly varying state of the environment. This procedure is based on contrastive loss, which pulls embeddings of nearby observations to each other while pushing away other samples from the batch. It can be interpreted as a metric that captures the temporal relations of observations. We propose to combine both common instantaneous and our history representation and we evaluate TempAI on all available Atari games from the Arcade Learning Environment. TempAI surpasses the instantaneous-only baseline in 35 environments out of 49. The source code of the method and of all the experiments is available at <https://github.com/htdt/tempal>.

## I. INTRODUCTION

Deep Reinforcement Learning (RL) algorithms have been successfully applied to a range of challenging domains, from video games [1] to a computer chip design [2]. These approaches use a Neural Network (NN) both to represent the current observation of the environment and to learn the agent’s optimal policy, used to choose the next action. For instance, the state observation can be the current game frame or an image of the robot camera, and a Convolutional Neural Network (CNN) may be used to obtain a compact feature vector from it.

However, often RL environments are only partially observable and having a significant representation of the past may be crucial for the agent [3]. For instance, in the Atari 2600 Pong game, the state must be represented as at least two consecutive frames. In this way, the agent can determine both the position of the ball and the direction of its movement. More complex partially observable domains require a longer state history input to the agent. For instance, when navigating inside a 1-st person-view 3D labyrinth, the agent obtains little information from the current scene observation and needs several previous frames to localise itself.

A common solution to represent the observation history is based on the Recurrent Neural Networks (RNNs), where the RNN hidden-layer activation vector is input to the agent, possibly together with the current state observation [4]. However,

RL is characterized by highly nonstationary data, which makes training unstable [5] and this instability is exacerbated when a recurrent network needs to be simultaneously trained to extract the agent’s input representation. In this case, the network must obtain the representation of multiple high-dimensional input frames supervised with only the reward signal. This results in a long, very computationally demanding training.

In this paper, we propose a different direction, in which the agent’s observation history is represented using compact embeddings, which describe a general state of the world. Environment-specific embeddings are trained in parallel with the RL agent using the common self-supervised contrastive learning method. Being low-dimensional, the embeddings are input directly to train the policy, indicating the most important changes in the past. Intuitively, this is inspired by the common human behaviour: when making decisions, humans do not keep detailed visual information of the previous steps. For instance, while navigating through the halls of a building, it is sufficient to recall a few significant landmarks seen during the walk, e.g. specific doors or furniture.

Following this idea, in this paper, we propose a Temporal Alignment for History Representation (TempAI) approach, composed of 3 iterative stages: *experience collection*, *temporal alignment* and *policy optimisation*. We obtain the representation by aligning past state observations using the pairwise cross-entropy loss function [6], [7]. In more detail, we minimize the distance between the latent representations of temporally-close frames. This is a form of *self-supervision*, in which no additional annotation is needed for the representation learning, the network is trained to produce consistent embeddings for semantically similar input (positives), contrasting them with other, more distant samples (negatives) [6], [8]–[10].

Once the observations have been aligned, the embedding of a given frame is used as the semantic representation of the observation and is recorded in a longer *history*. Finally, the history is input to the agent together with an *instantaneous* observation representation, obtained, following [1], as a stack of the last 4 frames. This information is now used for policy optimisation. Note that our proposed history representation is independent of the specific RL approach. However, in all our experiments we use the PPO algorithm [11] for the policy and the value function optimisation. The 3 stages are iterated during training, and thus past embeddings can be modified

<sup>§</sup>This work was done at DISI, University of Trento

and adapted to address new observations, while the agent is progressing through the environment.

We summarize the contribution of this paper below. First, we use the pairwise cross-entropy loss function [6], [7] to align the agent’s past observations and to obtain low-dimensional embeddings. Second, we represent the state of the agent with multiple previous observations as embeddings, so far trained. Finally, we combine both instantaneous and history representation and we evaluate our method using the PPO algorithm on all available 49 Atari games from the Arcade Learning Environment (ALE) [12] benchmark. Our experiments confirm that this combination provides a significant boost with respect to the most common instantaneous-only input. Specifically, we show that TempAI outperforms the baseline in cases, where the history can increase observability. The source code of the method and of all the experiments is available at <https://github.com/htdt/tempal>.

## II. RELATED WORK

### A. Partially Observable Markov Decision Processes

The goal of the agent is to maximize a cumulative reward signal and it interacts with the environment to achieve it. The interaction process is defined as a Partially Observable Markov Decision Process (POMDP)  $\langle S, A, T, R, \Omega, O, \gamma \rangle$  [13], [14], where  $S$  is a finite state space,  $A$  is a finite action space,  $R(s, a)$  is the reward function,  $T(\cdot|s, a)$  is the transition function,  $\Omega$  is a set of possible observations,  $O$  is a function which maps states to probability distributions over observations and  $\gamma \in [0, 1)$  is a discount factor used to compute the cumulative discounted reward. Within this framework, at each step  $t$ , the environment is in some unobserved state  $s \in S$ . When the agent takes an action  $a$ , the environment transits to the new state  $s'$  with probability  $T(s'|s, a)$ , providing the agent with a new observation  $o' \in \Omega$  with probability  $O(o'|s')$  and reward  $r \sim R(s, a)$ .

POMDPs are an active research area and several approaches have been recently proposed to address partial observability. DQN [1] is one of the earliest deep RL models directly trained using the high-dimensional observation  $o_t$  as input (i.e., the raw pixels of the current frame). To deal with partial observability, the input of the model is composed of a stack of the 4 last grayscale frames, processed as 4 channels using a 2D CNN. We also use this observation representation which we call *instantaneous* to highlight the difference from the past observation history.

[15] replace the fully-connected (FC) layer in DQN with an LSTM [16] layer. At each step, the model receives only one frame of the environment together with the LSTM hidden-layer value which represents the past. The idea was extended in [17] by inferring latent belief states. To simulate reduced observability and demonstrate the robustness of the method, [15] introduce the flickering Atari games, obscuring the observation with a certain probability at each step. These methods focus on short-term partial observability, such as noisy observations, and approximate the state with an implicitly inferred continuous history. In contrast, our method explicitly represents each

step of the past using an independently trained encoder, and concatenates a sequence of steps into a history. Our final goal is to augment the current state representation with important past changes of the environment.

Recurrent layers (e.g. LSTM or GRU [18]) are a common choice for modern RL architectures. The A3C algorithm [4] showed a high mean performance with an LSTM layer. R2D2 [3] is specifically focused on processing long-history sequences (80 steps with additional 40 burn-in steps) using an LSTM. However, despite its widespread, RNNs have disadvantages within an RL framework because they increase the training complexity (Sec. I). In this paper, we propose a compact history representation that can be processed with much simpler networks. In our experiments, we use a small 1D CNN with kernel size 1, which has only 68 trainable parameters. We empirically show in Sec. IV-D that our proposal improves the performance for most of the environments.

### B. Self-supervised Learning and Metric Learning

In this section we present related works focused on representation learning. In self-supervised learning (SSL), the network is trained to extract useful representations from data (e.g. images, videos) based on a *pretext task* without using annotation. In RL, observations are obtained dynamically, thus labeling them is impractical, while a suitable pretext task may require minimal effort. CPC [6] is a pioneering SSL method, that was demonstrated on natural images and in the RL domain. For images, the method predicts the representation of a patch given a context obtained from other patches. For RL, the method predicts the representation of an observation given previous observations in a sequence, and the SSL loss is combined as auxiliary with the RL loss. Similarly, our method uses temporal positions in the trajectory. However, we explicitly align the latent representation instead of prediction, and we do not combine losses, performing each stage separately.

[6] have introduced the InfoNCE loss, which became a foundation for several popular methods. E.g., MoCo [9] and SimCLR [10] use this loss to align representations of two versions of one image, produced by random augmentations (cropping, color jitter etc.). Later, several alternative non-contrastive losses were proposed [19]–[22]. However, in our setting InfoNCE provides better stability, we employ it for our experiments. In parallel with SSL, this loss was developed for metric learning, it was introduced as N-pair loss [23] and pairwise cross-entropy loss [7] emphasizing the connection with the cross-entropy loss for supervised classification.

Following CPC concepts, ST-DIM [8] used both patch structure and temporal positions of observations, aligning nearby frames. The method was validated on several Atari games from ALE measuring if the specific information from the environment is encoded in the representation; the RL task was not considered. Recently, [24] have shown that the self-supervision from temporal positions and from augmentations can improve data efficiency in RL, using BYOL [19] as an auxiliary loss.

SSL is widely adopted in world models. The goal of such models is to capture world dynamics, and it is often unreasonable to spend the model capacity predicting all pixel-level details. Thus, in World Models [25], observations are initially encoded with VAE [26] and the model operates in the resulting low-dimensional space. [27] have utilised temporal alignment of observations to learn latent space, and the world model approximates dynamics in this space to address the exploration problem. [28] extend model-based MuZero [29] with the self-supervised consistency for nearby observations based on SimSiam [21] loss, demonstrating the high sample efficiency. Differently from these works, TempAI is used in the model-free setting.

Our representation learning process can be viewed from the metric learning perspective. Metric is defined as a distance between objects representing their specific similarity. At the same time, TempAI representation indicates the temporal distance between observations. This idea was developed in Time-Contrastive Networks [30]. To obtain positives, one of the versions of the method used the temporal window as in III-A. The performance was demonstrated in a robotic imitation setting. Moreover, several prior works [31], [32] used temporal coherence for representation learning and our method can be seen as a continuation of this line of research.

### III. TEMPORAL ALIGNMENT AND HISTORY REPRESENTATION

#### A. Temporal Alignment

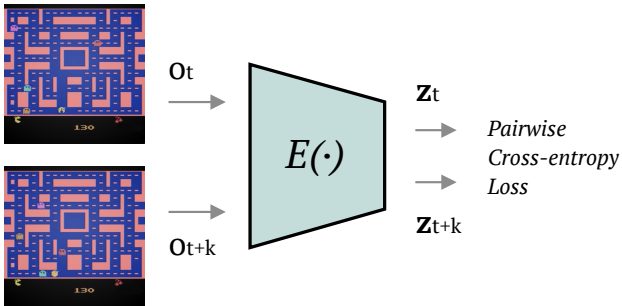


Fig. 1. Scheme of the temporal alignment. First, two frames are sampled within the temporal window  $L$  from one trajectory. They are encoded with  $E(\cdot)$ , which consists of a CNN with an FC layer and  $L_2$  normalization. Finally, the resulting embeddings  $\mathbf{z}_t$  and  $\mathbf{z}_{t+k}$  are pulled closer to each other, while other samples in the batch are pushed away using the pairwise cross-entropy loss.

As mentioned in Sec. I-II, for our self-supervised representation learning, we use the *pairwise cross-entropy loss*, which is a variant of the *contrastive loss* [33]. Following the common formulation proposed by [6]:

$$L_{cross-entropy} = -\log \frac{\exp(\mathbf{z}_i^T \mathbf{z}_j / \tau)}{\sum_{k=1, k \neq i}^K \exp(\mathbf{z}_i^T \mathbf{z}_k / \tau)}, \quad (1)$$

where  $\mathbf{z}$  is a latent-space representation of corresponding observation  $o$ , indexes  $i$  and  $j$  indicate a *positive* pair,  $K$  is the size of the current batch,  $\tau$  is a temperature hyperparameter.

Temporally-close observations share the same general state of the environment, while distant observations are likely to represent different states. Following this assumption, we use nearby observations as positives. Let  $o_t$  be the observation of the environment at time step  $t$ , presented as an image. We want to learn a representation mapping  $E(o_t) = \mathbf{z}_t$ ,  $E(\cdot)$  is our *self-supervised encoder* and it is based on a CNN [1] followed by a FC layer with  $L_2$  normalization (Fig. 1). We use two observations extracted from the same trajectory:  $o_t$  and  $o_{t+k}$ , where  $k \sim U[1, L]$ .  $L$  defines a temporal translation window in which observations are assumed to most likely have the same semantic content. Small values of  $L$  (e.g.  $L = 1$ ) reduce the uncertainty and thus improve the stability during training. However, if this value is too small, positives can often be identical and the encoder would be trained to simply detect duplicates. On the other hand, larger values of  $L$  produce a higher variability, in which the representation learning process is forced to extract more abstract semantics to group similar frames. During preliminary experiments, we observed that the optimal value lies in the range (1, 10) depending on the environment. On average, value  $L = 4$  provides the best result, thus we use it in our experiments in Sec. IV-D. However, it's possible to tune this parameter independently for each environment. Another parameter is the representation dimensionality  $dim(\mathbf{z})$ . We set it to 32 for all experiments, in considered cases it is sufficient. Additionally, inspired by the commonly used random crop augmentation in self-supervised learning [10], we randomly shift the image vertically and horizontally by the value from the range  $(-4, 4)$ , improving the encoder robustness.

#### B. History Representation and Policy Optimisation

Once  $E(\cdot)$  is updated (see Sec. IV-A), we use  $\mathbf{z}_t = E(o_t)$  to represent an observation at time  $t$  and update the agent's policy. In more detail, we represent the agent with an Actor-Critic architecture approximated with a NN  $\Theta$ . We use the PPO [11] algorithm to optimise the policy and the value function. At time step  $t$ , the agent receives two types of data as input, an *instantaneous* representation  $I(t)$  consisting of 4 concatenated raw-pixel, grayscale frames  $I(t) = \{o_t, o_{t-1}, o_{t-2}, o_{t-3}\}$  and a *history* computed with  $E(\cdot)$  over the past  $N$  steps:  $H(t) = \{\mathbf{z}_t, \dots, \mathbf{z}_{t-N+1}\}$ .  $\mathbf{z}_t$  is a low-dimensional vector (32), and the history size  $N$  can be set to a specific value depending on the environment (we use  $N = 16$ ), thus  $H(t)$  is a low-dimensional ( $32 \times 16$ ) matrix which represents significant information about the recent agent's past trajectory. Importantly, in contrast with an RNN-based history representation, which may be prone to forgetting past information, in our proposed history representation  $H(t)$ , all the past  $N$  observations are stored, together with their time-dependent evolution.

The NN  $\Theta$  consists of two branches with respect to the input: instantaneous and history. The instantaneous branch consists of a NN, introduced by [1] and commonly used for Atari in several works, including our baseline PPO. In the history branch the input  $H(t)$  is first passed through a 1D CNN with the kernel size 1, then flattened and processed

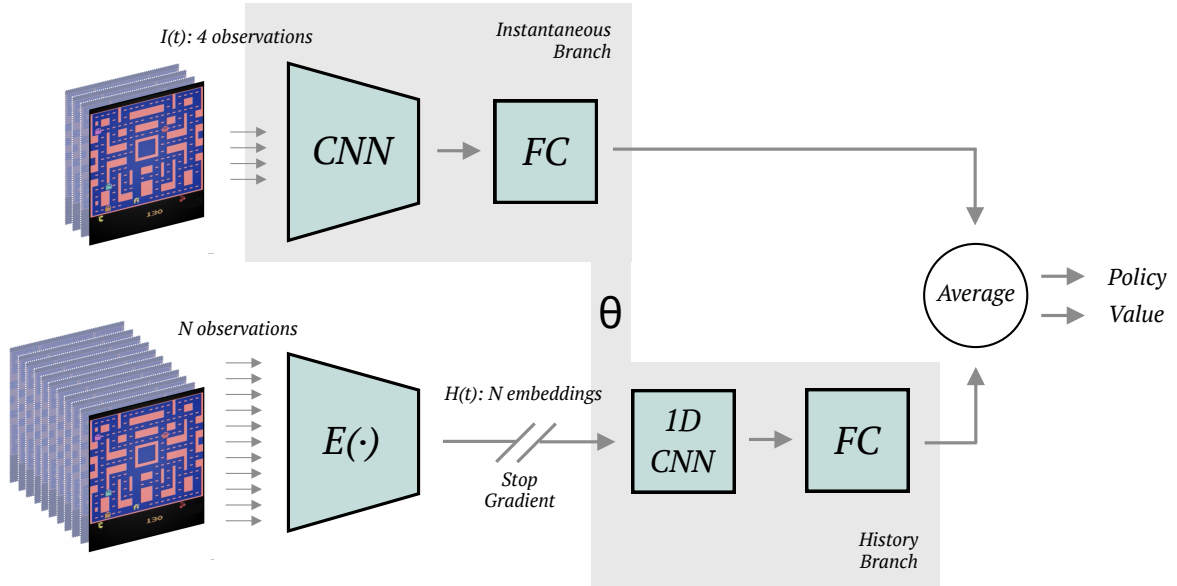


Fig. 2. Scheme of the RL agent architecture. The NN  $\Theta$  consists of two branches: instantaneous and history. The former is a common RL architecture, which processes four recent observations and outputs policy probabilities and the state value. The latter is designed to process embeddings of  $N$  history steps. First, these embeddings are obtained from the encoder  $E(\cdot)$ . Next, they are processed in the history branch, which predicts the policy and value in the same format as the instantaneous branch. Finally, both branches are ensembled and the output is optimized with the PPO algorithm. Note that in this scheme only the NN  $\Theta$  is updated, the encoder  $E(\cdot)$  is frozen during the policy optimisation stage.

with two FC layers. In this branch, we use two sub-networks with described architecture, one for the policy and one for the value. Finally, outputs of both branches are combined using an average. Such a basic ensembling allows the agent to choose a suitable input for a concrete task. We also include ablation studies (IV-E) with only the history branch. Fig. 2 shows the full architecture of our agent.

We highlight that the self-supervised encoder  $E(\cdot)$  does not share parameters with the RL network  $\Theta$ , and it is not trained during the policy optimisation stage. Moreover, while the  $E(\cdot)$  encoder is trained in a self-supervised fashion, the CNN in  $\Theta$ , used to extract representation from  $I(t)$ , is trained *using the RL reward*. This emphasizes the complementary between the knowledge of the two networks, being the former based on extracting visual similarities in data that do not depend on the specific RL task, while the latter being trained as in a standard RL framework, focusing on details important for action selection.

## IV. EXPERIMENTAL EVALUATION

### A. Training

Initially, we run a random agent for a small number of steps (1% of the total budget) storing all obtained observations. Next, we train the  $E(\cdot)$  encoder using these observations for  $n_{pretrain}$  epochs. After this pretraining, the RL agent can use  $E(\cdot)$  to encode the history and it is ready for the main training loop. During it, we run the RL agent in several parallel environments for a predefined number of steps (one rollout). The actions are chosen according to the current policy (*observation collection stage*). Next, using the collected experience, we update  $E(\cdot)$  for  $n_{encoder}$  epochs (*temporal*

TABLE I  
CONFIGURATION

Embedding size ( $dim(\mathbf{z})$ )	32
History size $N$	16
Temporal window $L$	4
Maximal spatial shift	4
Number of epochs $n_{pretrain}$	2500
Number of epochs $n_{encoder}$	1
Number of epochs $n_{policy}$	3
Batch size (temporal alignment)	2048
Learning rate (temporal alignment)	$2 \times 10^{-4}$
Temperature $\tau$	0.1
Observations storage size	5120
1D CNN channels ( $\Theta$ history branch)	4
FC size ( $\Theta$ history branch)	128

*alignment stage*) and  $\Theta$  for  $n_{policy}$  epochs (*policy optimisation stage*). These three stages are iterated, so to adapt  $E(\cdot)$  to the observation distribution change.

### B. Implementation Details

The weights of  $E(\cdot)$  and  $\Theta$  are initialized with a (semi-) orthogonal matrix, as described in [34], and all the biases are initialized with zeros. We use one network architecture and one set of hyperparameters for all our experiments. We adopt the training procedure and the hyperparameters in [11], including the total number of time steps equal to 10M. Our agent network architecture is similar to [11], except for the

additional history branch. Encoder  $E(\cdot)$  is composed of a CNN and a FC layer (Sec. III-A). Specifically, its CNN configuration is similar to [1], except the first layer, which takes only one channel as input, which corresponds to one grayscale observation. In Tab. I we list all other hyperparameters.

Pairwise cross-entropy loss makes use of batch samples as negatives and the sampling procedure can affect the optimization process. If observations are sampled from very distant parts of the trajectory, separating them is trivial. And vice versa: batch sampled from a small window makes the problem unsolvable. In all our experiments we sample pairs from 5 last rollouts, each rollout contains 128 steps of 8 parallel environments.

### C. Environments

We evaluate TempAI on the challenging deep RL benchmark ALE [12]. Following closely the experimental protocol of the baseline [11], we use all 49 available classic Atari 2600 video games. In these environments,  $o_t$  is an RGB image. The action space is discrete and the number of actions varies in each game from 4 to 18. We apply the same observation pre-processing (frame downscaling, etc.) as in [11].

### D. Results

In all the experiments the scores are averaged over 100 episodes. Fig. 3 shows the relative improvement with respect to baseline [11]. It is calculated as

$$\frac{R_{TempAI} - R_{random}}{R_{instant} - R_{random}} - 1, \quad (2)$$

where  $R_{TempAI}$  is the final cumulative reward of our method,  $R_{random}$  is the reward of a random agent, and  $R_{instant}$  is the reward of the baseline [11]. We can see that there is performance improvement in 35 out of 49 environments. A small difference with the baseline indicates that the game is likely reactive and the history does not add information. Large negative values indicate failure cases (3 environments), where the history input interferes with the instantaneous input. Finally, for 14 environments we can see a strong improvement ( $> 50\%$ ), in these cases, the history provides a clear advantage for the RL algorithm.

Additionally to quantitative results, we include the visualisation of the resulting embeddings in Fig. 4. We use a trajectory of the agent after training in `MsPacman` environment. Each observation is encoded with  $E(\cdot)$  and then projected to 2D with the t-SNE [35] algorithm. We can see that observations are perfectly aligned and the encoder successfully learned the target representation. Interestingly, the curves of the path correspond to special events during the run. The game starts with an initial animation where the agent cannot move, so these frames (0 and 50) are bunched up. Similar animations are around points 700 and 800 after losing a life. After step 400 the agent takes a bonus which allows attacking opponents, this creates a gap with a twist in the path. Around step 550 the agent was trapped and it also results in a special twist.

It is important to note that our method requires an additional computational budget with respect to the baseline with only

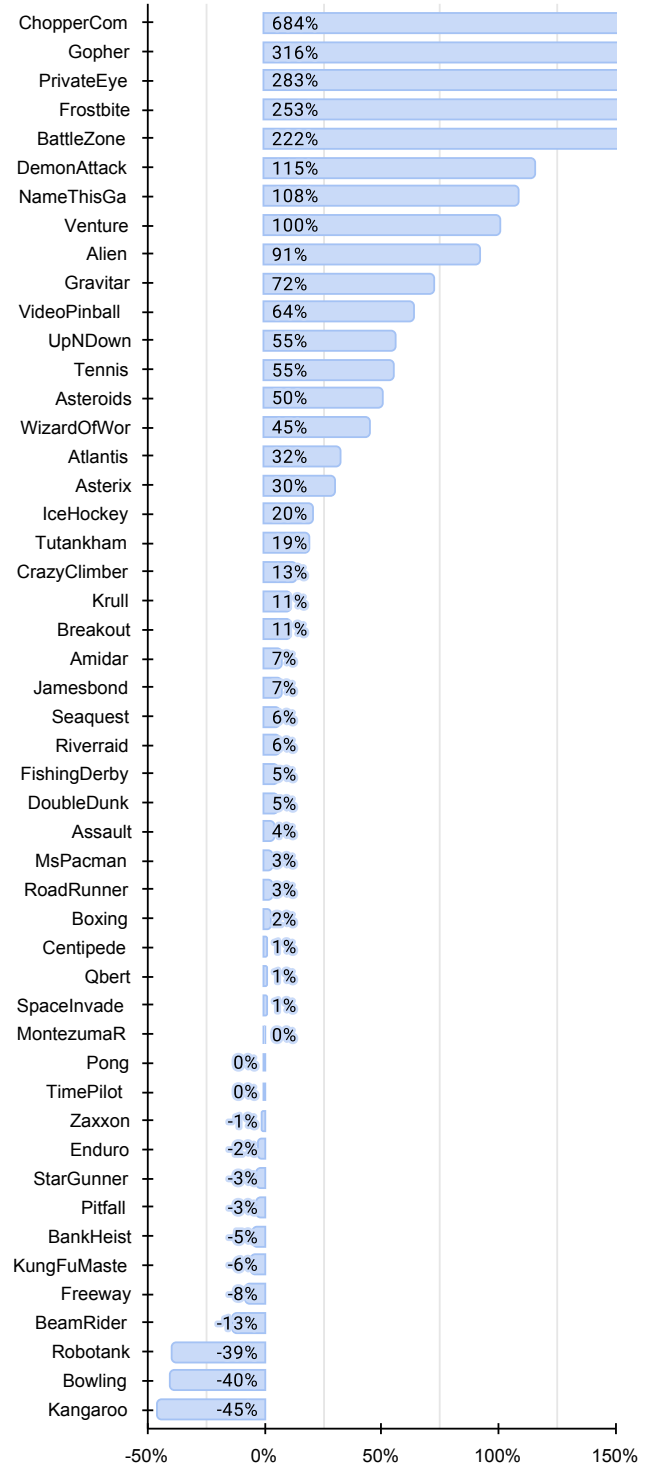


Fig. 3. Relative improvement (Eq. 2) of TempAI with respect to the baseline architecture with only the instantaneous input. 0% indicates that our method obtains the same cumulative reward as the baseline, while higher values indicate superior performance. Note that for `Venture`  $R_{random} = R_{instant} = 0$ , while  $R_{TempAI} = 35$ , the improvement is shown as 100%.

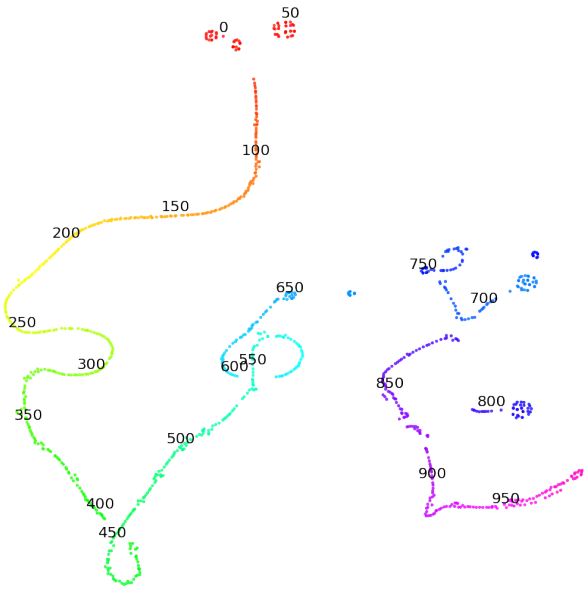


Fig. 4. Visualisation of the trajectory (1000 steps) of the agent in `MsPacman` environment. After training, the agent runs the obtained policy storing embeddings for each observation, produced by  $E(\cdot)$ . Then embedding are projected to 2D with the t-SNE algorithm. Nearby steps are depicted in a similar color, and the step counter shows specific points on the trajectory.

TABLE II  
FINAL AVERAGED CUMULATIVE REWARDS OF  
ABLATIVE VERSIONS OF THE AGENT

Environment	Random	History	Instant.	Ensemble
Asteroids	810.5	1360.7	2157.7	<b>2827.4</b>
Breakout	1.3	30.48	370.14	<b>409.42</b>
Freeway	0	30.58	<b>33.3</b>	30.7
Frostbite	74.7	276.1	293.8	<b>848.2</b>
Gravitar	194	448.5	455	<b>642</b>
MsPacman	237.6	<b>1895.3</b>	1840.9	1890.9
Seaquest	80.8	778.4	1739.4	<b>1843.6</b>
SpaceInvaders	133.4	521.45	1070.9	<b>1079</b>
Tennis	-23.9	-2.31	-9.43	<b>-1.49</b>

instantaneous input. The significant overhead comes from the temporal alignment stage and from producing embeddings for  $H(t)$  during the policy optimisation stage. However, the encoder  $E(\cdot)$  does not depend on the goal or the reward, so in a more realistic setting, we can train it once for the environment and reuse it for different tasks. In addition, if the encoder is not updated, the embeddings can be stored during experience collection, neglecting the corresponding overhead during the policy optimisation.

#### E. Ablation study

Most Atari environments are reactive, e.g. in `Breakout`, it is important to catch the ball precisely. In such cases, instantaneous input is favorable, while using only compact

history may be not sufficient. We verify this assumption in the following experiment. We remove the instantaneous branch and corresponding input, and we use only the history branch. The only modification of hyperparameters is a bigger size of the FC layer 512. Tab. II shows all the considered versions. The history-only method performs better than random, thus the agent was able to extract necessary information in every environment. In some cases the performance of history-only and instantaneous-only methods is similar, the history representation is sufficient. However, the ensemble shows the best result combining the advantages of both types of input.

## V. CONCLUSION

We presented a method for history representation in RL. Our TempAI is based on the idea that important information about the past can be “compressed” using temporal alignment of observations. Specifically, this representation is learned using the common SSL approach based on the pairwise cross-entropy loss. The encoder and the agent are trained jointly and iterated through time, to adapt the history representation to the new observations.

In TempAI, visual information is represented using two different networks: the SSL encoder  $E(\cdot)$  and the RL agent  $\Theta$ . The latter is trained using a reward signal, so it presumably extracts task-specific information from the observations. On the other hand, the encoder  $E(\cdot)$  is trained using self-supervision, and thus it focuses on patterns that are repeated in the data stream, potentially leveraging a larger quantity of supervision signal. Although SSL has been explored in other RL and non-RL works, this is the first work to show how the discovered information can be exploited in the form of history representation.

**Broader Impact.** Our approach was demonstrated on Atari games, the most popular RL benchmark with image observations. This benchmark allows to run numerous simulations quickly, thus experiments can be carried out with a reasonable budget. However, simple sprite-based computer graphics, used in these games, is only a rough proxy to real-world problems. On the other hand, SSL has recently enjoyed remarkable success in the natural image domain [10], [19]. Our representation learning is based on SSL, therefore TempAI can be used in environments with natural observations, e.g. in robotics. Furthermore, in some cases, TempAI can be pretrained from an unsupervised stream of observations, and later the encoder can be reused for other tasks in the environment since it does not depend on the reward. Moreover, real-world environments are often partially observable, e.g. in navigation, and the agent would benefit from the history input. We believe that our work can inspire further experimentation, advancing RL to practical applications.

## ACKNOWLEDGMENT

This work was supported by the EU H2020 AI4Media Project under Grant 951911.

## REFERENCES

- [1] V. Mnih, K. Kavukcuoglu, D. Silver, A. Graves, I. Antonoglou, D. Wierstra, and M. Riedmiller, "Playing atari with deep reinforcement learning," in *NIPS Deep Learning Workshop*, 2013.
- [2] A. Mirhoseini, A. Goldie, M. Yazgan, J. W. Jiang, E. Songhori, S. Wang, Y.-J. Lee, E. Johnson, O. Pathak, A. Nazi, J. Pak, A. Tong, K. Srinivasa, W. Hang, E. Tuncer, Q. V. Le, J. Laudon, R. Ho, R. Carpenter, and J. Dean, "A graph placement methodology for fast chip design," *Nature*, vol. 594, no. 7862, pp. 207–212, Jun 2021.
- [3] S. Kapturovski, G. Ostrovski, W. Dabney, J. Quan, and R. Munos, "Recurrent experience replay in distributed reinforcement learning," in *ICLR*, 2019.
- [4] V. Mnih, A. P. Badia, M. Mirza, A. Graves, T. P. Lillicrap, T. Harley, D. Silver, and K. Kavukcuoglu, "Asynchronous methods for deep reinforcement learning," in *ICML*, 2016.
- [5] J. Schulman, P. Moritz, S. Levine, M. I. Jordan, and P. Abbeel, "High-dimensional continuous control using generalized advantage estimation," in *ICLR*, 2016.
- [6] A. v. d. Oord, Y. Li, and O. Vinyals, "Representation learning with contrastive predictive coding," *arXiv preprint arXiv:1807.03748*, 2018.
- [7] M. Boudiaf, J. Rony, I. M. Ziko, E. Granger, M. Pedersoli, P. Piantanida, and I. B. Ayed, "A unifying mutual information view of metric learning: cross-entropy vs. pairwise losses," in *European conference on computer vision*. Springer, 2020, pp. 548–564.
- [8] A. Anand, E. Racah, S. Ozair, Y. Bengio, M.-A. Côté, and R. D. Hjelm, "Unsupervised state representation learning in atari," *Advances in Neural Information Processing Systems*, vol. 32, 2019.
- [9] K. He, H. Fan, Y. Wu, S. Xie, and R. Girshick, "Momentum contrast for unsupervised visual representation learning," in *Proceedings of the IEEE/CVF conference on computer vision and pattern recognition*, 2020, pp. 9729–9738.
- [10] T. Chen, S. Kornblith, M. Norouzi, and G. Hinton, "A simple framework for contrastive learning of visual representations," in *International conference on machine learning*. PMLR, 2020, pp. 1597–1607.
- [11] J. Schulman, F. Wolski, P. Dhariwal, A. Radford, and O. Klimov, "Proximal policy optimization algorithms," *arXiv preprint arXiv:1707.06347*, 2017.
- [12] M. G. Bellemare, Y. Naddaf, J. Veness, and M. Bowling, "The arcade learning environment: An evaluation platform for general agents," *Journal of Artificial Intelligence Research* 47, vol. 47, pp. 253–279, 2012.
- [13] G. E. Monahan, "State of the art—a survey of partially observable markov decision processes: Theory, models, and algorithms," *Management Science*, vol. 28, no. 1, pp. 1–16, Jan. 1982.
- [14] L. P. Kaelbling, M. L. Littman, and A. R. Cassandra, "Planning and acting in partially observable stochastic domains," *Artificial Intelligence*, vol. 101, no. 1, pp. 99 – 134, 1998.
- [15] M. Hausknecht and P. Stone, "Deep recurrent q-learning for partially observable mdps," in *2015 aaai fall symposium series*, 2015.
- [16] S. Hochreiter and J. Schmidhuber, "Long short-term memory," *Neural Computation*, vol. 9, no. 8, pp. 1735–1780, 1997.
- [17] M. Igl, L. Zintgraf, T. A. Le, F. Wood, and S. Whiteson, "Deep variational reinforcement learning for pomdps," in *International Conference on Machine Learning*. PMLR, 2018, pp. 2117–2126.
- [18] K. Cho, B. van Merriënboer, C. Gulcehre, D. Bahdanau, F. Bougares, H. Schwenk, and Y. Bengio, "Learning phrase representations using rnn encoder-decoder for statistical machine translation," in *EMNLP*, 2014.
- [19] J.-B. Grill, F. Strub, F. Altché, C. Tallec, P. Richemond, E. Buchatskaya, C. Doersch, B. Avila Pires, Z. Guo, M. Gheshlaghi Azar *et al.*, "Bootstrap your own latent—a new approach to self-supervised learning," *Advances in Neural Information Processing Systems*, vol. 33, pp. 21 271–21 284, 2020.
- [20] A. Ermolov, A. Siarohin, E. Sangineto, and N. Sebe, "Whitening for self-supervised representation learning," in *International Conference on Machine Learning*. PMLR, 2021, pp. 3015–3024.
- [21] X. Chen and K. He, "Exploring simple siamese representation learning," in *Proceedings of the IEEE/CVF Conference on Computer Vision and Pattern Recognition*, 2021, pp. 15 750–15 758.
- [22] J. Zbontar, L. Jing, I. Misra, Y. LeCun, and S. Deny, "Barlow twins: Self-supervised learning via redundancy reduction," in *International Conference on Machine Learning*. PMLR, 2021, pp. 12 310–12 320.
- [23] K. Sohn, "Improved deep metric learning with multi-class n-pair loss objective," in *Advances in Neural Information Processing Systems*, vol. 29. Curran Associates, Inc., 2016.
- [24] M. Schwarzer, A. Anand, R. Goel, R. D. Hjelm, A. Courville, and P. Bachman, "Data-efficient reinforcement learning with self-predictive representations," *arXiv preprint arXiv:2007.05929*, 2020.
- [25] D. Ha and J. Schmidhuber, "Recurrent world models facilitate policy evolution," in *Advances in Neural Information Processing Systems*, S. Bengio, H. Wallach, H. Larochelle, K. Grauman, N. Cesa-Bianchi, and R. Garnett, Eds., vol. 31. Curran Associates, Inc., 2018.
- [26] D. P. Kingma and M. Welling, "Auto-encoding variational bayes," in *ICLR*, 2014.
- [27] A. Ermolov and N. Sebe, "Latent world models for intrinsically motivated exploration," in *Advances in Neural Information Processing Systems*, H. Larochelle, M. Ranzato, R. Hadsell, M. F. Balcan, and H. Lin, Eds., vol. 33. Curran Associates, Inc., 2020, pp. 5565–5575.
- [28] W. Ye, S. Liu, T. Kurutach, P. Abbeel, and Y. Gao, "Mastering atari games with limited data," *Advances in Neural Information Processing Systems*, vol. 34, 2021.
- [29] J. Schrittwieser, I. Antonoglou, T. Hubert, K. Simonyan, L. Sifre, S. Schmitt, A. Guez, E. Lockhart, D. Hassabis, T. Graepel, T. Lillicrap, and D. Silver, "Mastering atari, go, chess and shogi by planning with a learned model," *Nature*, vol. 588, no. 7839, pp. 604–609, Dec 2020.
- [30] P. Sermanet, C. Lynch, Y. Chebotar, J. Hsu, E. Jang, S. Schaal, S. Levine, and G. Brain, "Time-contrastive networks: Self-supervised learning from video," in *2018 IEEE international conference on robotics and automation (ICRA)*. IEEE, 2018, pp. 1134–1141.
- [31] L. Wiskott and T. J. Sejnowski, "Slow feature analysis: Unsupervised learning of invariances," *Neural Comput.*, vol. 14, no. 4, p. 715–770, 2002.
- [32] R. Goroshin, J. Bruna, J. Tompson, D. Eigen, and Y. LeCun, "Unsupervised learning of spatiotemporally coherent metrics," 2015.
- [33] R. Hadsell, S. Chopra, and Y. LeCun, "Dimensionality reduction by learning an invariant mapping," in *CVPR*, 2006.
- [34] A. M. Saxe, J. L. McClelland, and S. Ganguli, "Exact solutions to the nonlinear dynamics of learning in deep linear neural networks," 2014.
- [35] L. van der Maaten and G. Hinton, "Visualizing data using t-SNE," *Journal of Machine Learning Research*, vol. 9, pp. 2579–2605, 2008.